

Can positrons provide defect spectroscopy in special alloys such as reactor steels? An assessment

This article has been downloaded from IOPscience. Please scroll down to see the full text article.

1989 J. Phys.: Condens. Matter 1 SA71

(<http://iopscience.iop.org/0953-8984/1/SA/009>)

View [the table of contents for this issue](#), or go to the [journal homepage](#) for more

Download details:

IP Address: 129.252.86.83

The article was downloaded on 27/05/2010 at 11:09

Please note that [terms and conditions apply](#).

Can positrons provide defect spectroscopy in special alloys such as reactor steels? An assessment

B Viswanathan

Materials Science Division, Indira Gandhi Centre for Atomic Research, Kalpakkam
603 102, India

Received 7 December 1988, in final form 16 March 1988

Abstract. The question as to whether positron studies can provide a detailed and quantitative understanding of defect properties in special alloys, such as reactor steels, is examined with specific reference to helium effects in irradiated materials. On the basis of our recent understanding of positron states in gas bubbles, the positron lifetimes in α -irradiated stainless steel are analysed to deduce parameters such as helium atom density, bubble radius and bubble concentration. These deduced bubble parameters are compared with independent TEM results on the alloy. The determination of activation energy for bubble growth at high annealing temperatures is discussed. The effect of Ti-alloying on bubble growth in Ni (chosen as the model metal for steel) is discussed with reference to positron results in NiTi alloys. Finally, a comparative assessment is made of the positron method in relation to other prevailing techniques in the study of helium in metals.

1. Introduction

Austenitic stainless steel and its modified alloy forms are candidate materials for fuel cladding in fast reactors and the first plasma containment wall in fusion machines [1, 2]. Helium generation during irradiation is particularly high in fusion reactor materials (~ 300 PPM a^{-1}), since the 14 MeV neutrons escaping the plasma wall produce He by (n, α) reaction. The key property governing the behaviour of helium in materials is its extremely low solubility leading to precipitation in bubbles and helium embrittlement.

Positron annihilation spectroscopy (referred to as PAS) is a powerful technique capable of providing detailed understanding of vacancy-type defects in metals and alloys [3]. Recent developments [4] on the study of positron states in gas bubbles have shown that positron lifetime is markedly sensitive to: (i) the size and helium-to-vacancy ratio of small clusters and (ii) the helium atom density (pressure) in large bubbles. The latter connection between positron lifetime and gas density has led to a detailed analysis of bubble parameters on the basis of positron data in Al [5] and Cu [6]. We extend the analysis, as discussed below, to the study of helium-implanted austenitic stainless steel and NiTi alloys. The PAS results are compared with independent transmission electron microscopy (TEM) results. A comparative assessment is also made.

2. Alpha-irradiated austenitic stainless steel (SS316)

In a recent study carried out by the author and his collaborators [7], helium was homogeneously implanted at ambient temperature to a depth of 100 μm in austenitic stainless steel of type 316 (at.% Fe 65, Ni 12, Cr 18, Mo 1.4) to a dose of 500 atomic ppm,

Table 1. Deduced bubble parameters from an analysis discussed in § 2 for helium-irradiated SS316. (Uncertainty in $P_\tau \sim 20\%$.) T_{ann} is the annealing temperature; other symbols are defined in § 2.

T_{ann} (K)	τ_2 [7] (ps)	n_{He} (nm ⁻³)	P_τ (MPa)	P_{eq} (MPa)
1000	285	56	2080	1400
1050	310	45.5	1260	1040
1100	320	41.5	1040	925
1150	330	38.0	885	755

using high-energy α -particles from a cyclotron. An investigation of the post-irradiation evolution of the defect structure was made by monitoring the correlated behaviour of positron lifetime and Doppler lineshape [7]. The bubble nucleation temperature in SS316 was deduced as 750 ± 50 K. Post-nucleation growth of bubbles, as revealed by positron measurements, has been confirmed by independent TEM measurements [8].

We take up an analysis of the positron lifetime data in [7] corresponding to the grown bubbles in SS316. According to the model of Jensen and Nieminen [4], the stable positron state is at the bubble surface, i.e. at the He-metal interface. The positron lifetime is the sum of contributions from constant annihilation rate with metal electrons at the interface and a density-dependent annihilation rate with He electrons. The established relation (referred to as the J-N relation) connecting helium atom density n_{He} and lifetime τ does not seem to depend on the specific nature of the metal in question. Accordingly, the J-N relation has been applied to the case of stainless steel and n_{He} obtained from the experimental lifetime τ_2 in [7]. The corresponding helium pressure P_τ in the bubble at a given temperature has been deduced from n_{He} using the high-density equation of state [9]. The equilibrium bubble pressure $P_{\text{eq}} (=2\gamma/r_b)$ has been independently determined using the known value [10] of the surface energy γ for SS316 and bubble radius r_b obtained from TEM data [8]. The results for the deduced pressures are given in table 1 for different annealing temperatures. Within the uncertainties of the procedure used, there is fair agreement between P_τ and P_{eq} . This leads to the conclusion that the condensation of thermal vacancies on the bubble at high temperatures keeps the internal gas pressure in equilibrium with its surface tension. Hence the present results would support the vacancy mode of pressure relaxation in bubbles.

The bubble radius r_b and bubble concentration C_b are obtained from PAS data without introducing extra parameters [5, 6]. C_b can be obtained from the positron trapping rate K_b , which is known from the experimental lifetime parameters fitted to the standard trapping model [3]. To relate C_b and K_b , the specific trapping rate μ_b should be known. μ_b , in addition to being dependent on bubble size, is also weakly dependent on n_{He} . However, at our present level of understanding, the complete function $\mu(n_{\text{He}}, r_b, T)$ is not known. Hence, the crossover region between transition-limited positron trapping and diffusion-limited trapping is not clearly known in the case of bubbles. Accordingly, in the present study, μ_b as obtained from the semi-empirical relationship [11] for $\mu_b(r)$ is corrected for its small dependence on n_{He} . The latter correction is done by scaling μ_b by a factor which scales the variation of positron binding energy to the bubble with n_{He} [4]. This correction is of the order of 10% for the helium densities considered here. Knowing K_b and μ_b , C_b can be obtained. If the total He concentration in the sample N_{He} is assumed to be in bubbles (taken to be spherical), r_b is obtained from the helium inventory relation [5, 6] which connects r_b with N_{He} , n_{He} and C_b . The deduced radius r_b^{PAS} and concentration C_b^{PAS} are shown in figure 1 as a function of annealing temperature.

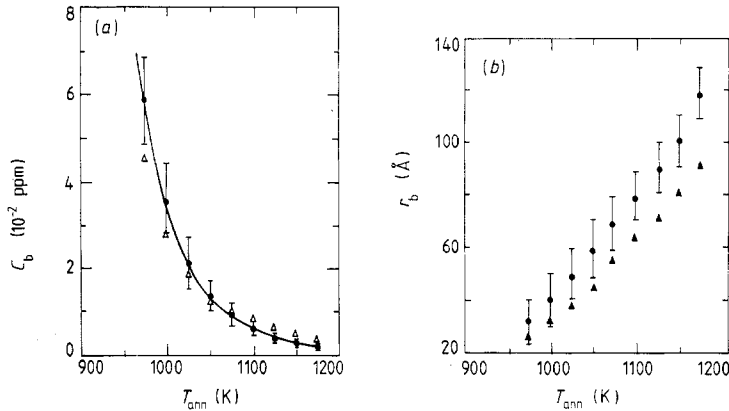


Figure 1. (a) Deduced bubble concentration C_b^{PAS} (●) from PAS data as a function of annealing temperature T_{ann} for helium-irradiated SS316; C_b^{TEM} (△) from TEM data is shown for comparison. (b) Deduced bubble radius r_b^{PAS} as a function of annealing temperature for helium-irradiated SS316; r_b^{TEM} (▲) from TEM data is shown for comparison.

The error bar shown in figure 1 is the estimate of total uncertainty ($\sim 25\%$) in the deduced parameters. r_b^{TEM} and C_b^{TEM} are also shown for comparison in figure 1. The agreement between the bubble parameters corresponding to PAS and TEM is considered satisfactory. However, the deviation noticed for the radii above 1100 K in figure 1 possibly arises from the over-estimate of r_b^{PAS} brought about by the assumption that there is no helium loss from bubbles.

The increase in r_b and decrease in C_b with temperature leads to the question of the mechanism of bubble coarsening. This is an unsolved issue under intense discussion [12, 13]. There are two distinct model mechanisms proposed for bubble coarsening. One involves bubble migration and coalescence [12] while the other is the Ostwald ripening process involving re-solution and permeation of He [13]. The average bubble radius in either case depends exponentially on temperature through the diffusion constant appropriate to the rate-limiting process. In the bubble coalescence model, the limiting process is governed by the activation energy for bubble diffusion. In the Ostwald ripening process, the activation enthalpy for growth can be identified as the sum of the free energy of solution for helium and the activation energy for its migration. This sum turns out to be 3.5 eV for stainless steel [13]. Figure 2 shows the Arrhenius plot of the deduced r_b^{PAS} in the present study; the plot for r_b^{TEM} is also shown for comparison. The activation energy for bubble coarsening deduced from the plot is $E_g = (1.25 \pm 0.35)$ eV. This value is smaller by a factor of 2 to 3, compared with the value of 3.5 eV expected for the Ostwald ripening mechanism. This disagreement seems to rule out the latter growth mechanism in the present case.

3. Effect of Ti-alloying on bubble growth in Ni

Titanium-modified stainless steel is a promising candidate as a helium-resistant alloy for reactor applications [14]. A systematic study of the effects of helium on this material is therefore imperative. As a first step towards this objective, PAS investigations have been carried out by the author and his co-workers [15] on NiTi alloys, with Ni chosen as the model metal for steel. The concentration of Ti used in the study [15] ranges from 0.5 at. % to 5 at. %, which is below the limit of solubility of Ti in Ni. The observed lifetimes characteristic of helium bubbles have been analysed by the same procedure discussed in

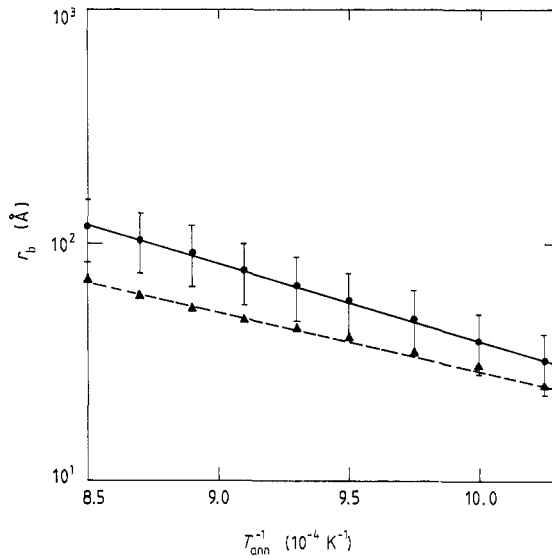


Figure 2. Arrhenius plot of bubble radius r_b against reciprocal annealing temperature for helium-irradiated SS316.

Table 2. Deduced bubble parameters for helium-irradiated Ni and NiTi alloys at the post-irradiation annealing temperature of 1120 K (see for details).

[Ti] (at. %)	τ_2 [15] (ps)	n_{He} (nm^{-3})	r_b^{PAS} (Å)	r_b^{eq} (Å)	C_b^{PAS} (10^{-3} ppm)
	380	24	99 ± 20	90	1.1
0.5	320	38	44 ± 9	38	6.8
1	300	45	42 ± 8	30	7.6
5	290	53	28 ± 6	25	10.0

§ 2. The results are shown in table 2 and figure 3. r_{eq} in table 2 refers to the bubble radius obtained by equating the pressure to the equilibrium value. As seen from both table 2 and figure 3, n_{He} and C_b are found to increase with Ti concentration. r_b is lower for the NiTi alloy, as compared with that in Ni, implying higher helium pressure brought about by the addition of Ti. These effects have been qualitatively understood in terms of enhanced helium trapping due to substitutional Ti impurity. Ti acts as an oversized impurity with smaller electron density in the host Ni. Such sites might be the preferential trapping centres for helium agglomeration. Consequently, an increase in the number of bubble nucleation sites and higher helium occupancy per site might result with the addition of Ti. Further work is in progress [15] with the aim of a complete understanding of the effect of Ti-alloying on bubble growth.

4. Comparison of PAS with other techniques

A brief comparative assessment of PAS in relation to other prevailing techniques will now be provided. The most direct determination of r_b and C_b is obtained from TEM. However, TEM is sensitive only to large bubbles and provides no direct information on the gas content inside the bubble. Small-angle x-ray and neutron scattering techniques are also sensitive to the size and concentration of large He-filled cavities. The merit of

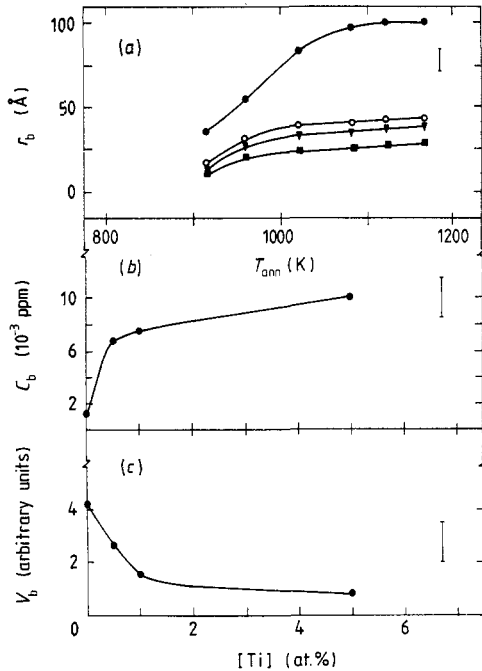


Figure 3. (a) Bubble radius r_b^{PAS} against annealing temperature for helium-irradiated Ni and NiTi alloys. (b) Bubble concentration C_b^{PAS} as a function of Ti concentration at the post-irradiation annealing temperature 1120 K. (c) Variation of bubble swelling as a function of Ti concentration corresponding to the annealing temperature 1120 K. V_b is the total bubble volume.

PAS for the study of helium lies in the fact that the method is sensitive to bubbles over a wide size range which includes the regions of incubation, nucleation and growth. Information on helium density, size and concentration can be obtained from PAS, as shown in the previous sections. A number of techniques such as electron energy-loss spectroscopy and vacuum ultraviolet absorption spectroscopy have been employed in recent times to determine He densities in bubbles [16]. These techniques, however, require thin films ($<1 \mu\text{m}$) with high concentration of He (a few at. %), whereas PAS is best suited for bulk samples ($\sim 100 \mu\text{m}$) with sensitivity to He concentrations as low as 1 appm. When using bulk samples, the determination of He density is not affected by any appreciable He loss to the sample surface. This is an advantage of PAS over other methods. The paramount importance of an accurate knowledge of pressure in bubble characterisation cannot be overemphasised [16]. Refinements on the current model schemes and more accurate knowledge of the dependences of positron lifetime and specific trapping rates ($\tau(n_{\text{He}}, r)$ and $\mu(n_{\text{He}}, r)$) should lead to the required precision in the bubble parameters from the present level of uncertainty.

In the small cluster regime, the perturbed angular correlation (PAC) technique provides a complementary role to PAS, as illustrated in a recent PAC study on stainless steel [17]. The temperature range and stability of small He complexes, as deduced from the characteristic hyperfine interaction parameters [17] seem to match well with the results [7] based on the variation of positron lifetimes. This suggests that a more complete and consistent description of the nucleation properties of microbubbles can be obtained by a combined study of PAS and PAC in a given material. Information on the binding energy of helium to lattice defects comes from yet another complementary technique, namely, thermal desorption spectroscopy.

Finally, it must be mentioned that PAS is not directly sensitive to bubbles at grain boundaries, unless the grain size is comparable to the average positron diffusion length. The grain size is usually large (several micrometres) in practical alloys under realistic

conditions. This raises a question as to whether PAS has any utility in the study of helium embrittlement and intergranular effects. The answer lies in the fact that quantitative determination of bubble parameters for the matrix or preferential locations such as precipitates (e.g. TiC), as obtained by PAS, can still be useful in determining the net helium flux and bubble population at grain boundaries. In this respect, PAS can be used indirectly to evaluate the susceptibility of engineering materials to helium embrittlement.

5. Summary and conclusions

In summary, the discussions in the earlier sections show how PAS can be an effective method for deriving qualitative as well as quantitative information on thermally activated nucleation and growth of helium bubbles in special alloys. The PAS study on NiTi alloys discussed in § 3 shows promise for investigating the effect of TiC precipitates on bubble formation in Ti-modified stainless steels, which are reactor materials of current importance. A detailed defect characterisation in ferritic steels, using PAS, is also needed. Such attempts on ferritic steels might be useful (with restricted scope) in assessing the susceptibility to helium embrittlement of reactor pressure vessel steels.

To conclude, a systematic approach with well specified material parameters, controlled experiments and correlation of PAS-based data with those from other complementary techniques in a given material, holds promise for providing a viable defect-spectroscopy in special alloys of technological importance.

Acknowledgments

The author expresses his great pleasure in presenting this paper at IPW88 held at Munchen, coinciding with the 50th birthday of Professor Dr W Triftshausen. His collaboration, and that of G Koegel, in the experiments on helium-implanted stainless steels is gratefully acknowledged. The author would also like to acknowledge the collaboration of Shri G Amarendra in the studies on NiTi alloys.

References

- [1] Ullmaier H and Schilling W 1980 *Physics of Modern Materials* vol 1 (Vienna: IAEA) pp 301–97
- [2] Ullmaier H 1984 *Nucl. Fusion* **24** 1039
- [3] Brandt W and Dupasquier A (ed.) 1983 *Positron Solid State Physics* (Amsterdam: North-Holland) p 196–401
- [4] Jensen K O and Nieminen R M 1987 *Phys. Rev. B* **36** 8219
- [5] Jensen K O, Eldrup M, Singh B N and Victoria M 1988 *J. Phys. F: Met. Phys.* **18** 1069
- [6] Viswanathan B, Amarendra G and Gopinathan K P 1988 *Radiat. Eff.* at press
- [7] Viswanathan B, Triftshausen W and Koegel G 1983 *Radiat. Eff.* **78** 231
- [8] Viswanathan B 1988 private communication
- [9] Trinkaus H 1983 *Radiat. Eff.* **78** 189
- [10] Thompson A W 1975 *Mater. Sci. Eng.* **21** 41
- [11] Jensen K O, Eldrup M, Singh B N, Horsewell A, Victoria M and Sommer W F 1987 *Mater. Sci. Forum* **15–18** 913
- [12] Goodhew P J and Tyler S K 1981 *Proc. R. Soc. A* **377** 151
- [13] Rothaut J, Schroeder H and Ullmaier H 1983 *Phil. Mag. A* **47** 781
- [14] Kesternich W 1985 *J. Nucl. Mater.* **127** 153
- [15] Amarendra G and Viswanathan B 1989 unpublished
- [16] Donnelly S E 1985 *Radiat. Eff.* **90** 1
- [17] Deicher M, Grubel G and Wichert Th 1983 *Nucl. Instrum. Methods* **209–10** 817